Measurement of the Dilatant Flow Properties of Some Non-Newtonian Suspensions

A. S. ROBERTS, Jr.[1]
Department of Mechanical Engineering, University of Pittsburgh, Pittsburgh, Pa.

Non-Newtonian fluid properties are usually exhibited by fine particle suspensions. This study is primarily concerned with the identification of dilatant suspensions, a specific non-Newtonian classification of fluids which shows increased apparent viscosity with increased shear rate. The suspension viscometer described was designed for measuring fluid shear of dilatant materials flowing in capillary tubes. Observed dilatant flow properties are given for two suspensions, and pseudoplastic behavior is recorded for one other sample.

INCREASED application of slurry and suspension flows, for example in nuclear reactor research where suspension coolants and fuels have been suggested, exemplifies the need for a broad spectrum of flow property data. Before pipes can be sized for prescribed efflux a sufficient knowledge of the flow properties of the fluid system must be established. In the case of non-Newtonian suspensions such data is not readily available. This paper presents the determination of two rheological flow parameters which have been used to describe dilatant suspensions, namely, n' and k', a flow behavior index and fluid consistency index, respectively. A rheometer was designed specifically for concentrated particle suspensions, and the analytical model of Metzner and Reed (8) was adopted for data interpretation.

INSTRUMENT DESIGN

The term "rheometer" has been introduced to describe an instrument used to study non-Newtonian as well as Newtonian fluid flow. Any instrument with this mission must provide a fluid shearing action in such a manner that the relative stress in the fluid is measurable and can be related to the rate at which this fluid shear progresses. A type of capillary instrument is adapted for this study in view of the simplicity of the mathematical model which is based on laminar flow in tubes.

There are several adequate rotational instruments available commercially. Unfortunately, there are few capillary rheometers on the market which are especially adapted for concentrated suspensions. Specialized tools such as extruders are available, but it is necessary to custom design a capillary instrument if particular design criteria are to be incorporated. Some basic criteria are listed below.

Close pressure control.
Fluid reservoir accomodating an adequate volume of material.
Capillary diameters ranging around 0.050 inch, lengths greater than 12 inches.
Temperature control of sample in the capillary and the reservoir.
Accurate measurement of flow rate (usually a stop watch and balances or volumetric catch vessel).

Good pressure control should allow the investigator a 10-fold shear-rate range. The reservoir is sized in a way so that the velocity of the fluid surface is negligible. Capillary lengths should be great enough to minimize end effects. While capillary diameters must be considerably larger than solid particle diameters, high stresses must be sustained in the laminar flow regime implying low Reynolds number and consequently small capillary diameter. Temperature control is important since the apparent viscosity varies strongly with changes in temperature—e.g., a 1°C. variation in the temperature of ambient water causes a 2% change in viscosity (5). To avoid the problem of inhomogeneity due to settling, a means of mechanically dispersing the solid phase is desirable in a well designed rheometer reservoir; however, such a device was omitted from our rheometer since freshly prepared samples were to be tested immediately.

Simplicity of design consistent with reasonable experimental accuracy was the guiding criterion. Gas pressure (nitrogen) was taken as the driving force in order to vary the fluid flow rate through the capillaries. The rheometer reservoir was consequently designed as a 300-p.s.i.g. pressure vessel. Figure 1 is an assembly drawing of the pressure vessel. Since the blind flange at the bottom is clear of bolt protrusions, the vessel could be arranged vertically upon a stand with the capillary centered and extending perpendicularly downward from the bottom of the vessel. Three vessel insertions were made through the top flange, for a pressure tap, a valving mechanism that moves vertically over the capillary protrusion, and a thermometer well. A mechanism for agitation within the vessel—e.g., a motor and paddle wheel—was not included since the above mentioned insertions were of greater importance. The vessel assembly was designed to rest on a stand, 8 inches above the floor of a constant temperature bath consisting of 16-inch diameter metal cylinder. This bath fitted into a fiber board cylinder which served to provide a 1-inch stagnant air gap about the perimeter of the bath. The entire system was conveniently located on a laboratory bench.

Calibration. In order to establish the validity of viscometric measurements made with the capillary rheometer, water and glycerol were used as calibrating samples. Some difficulty was encountered since the rheometer was not designed for low consistency materials; however, valid calibration measurements, which are mentioned subsequently, were determined. Successful operation of the rheometer depended particularly on clean capillary tubes, because foreign matter in the pressure vessel or capillary led inevitably to disrupted flow.

[1] Present address, Department of Nuclear Engineering, North Carolina State College, Raleigh, N. C.

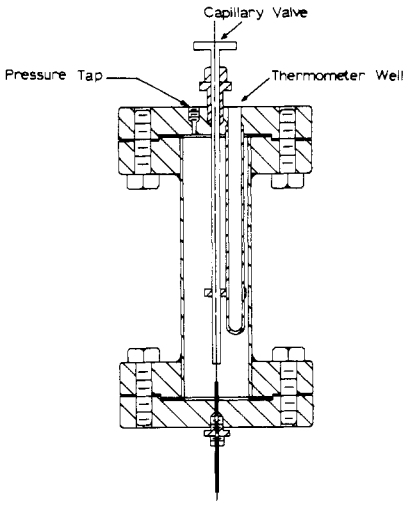

Figure 1. Pressure vessel assembly

Pressure drop caused by fluid shear in the capillary tubes was determined using the formula of Hagen-Poiseuille which was developed for laminar flow in circular tubes

$$\Delta P_f = 8\mu \frac{L\bar{u}}{r^2} \tag{1}$$

An additional pressure loss results when fluid enters the well-rounded entrance of a tube leading from a static fluid reservoir. This loss is composed of two parts; the $(\rho\bar{u}^2/2g_c)$ loss resulting when the fluid is accelerated in the entrance to the tube, the $(\rho\bar{u}^2/2g_c)$ loss incurred when the uniform velocity distribution at the tube entrance is transformed into a parabolic distribution (*10*). Hence,

$$\Delta P_T = 8\mu \frac{L\bar{u}}{r^2} + 2\left(\frac{\rho\bar{u}^2}{2g_c}\right) \tag{2}$$

is the pressure differential resulting between the reservoir and the end of a tube of length L in which there is a parabolic velocity distribution. The pressure applied to induce flow in the capillary is the gas pressure in the fluid reservoir, P_1, and the fluid elevation head, H. This pressure will be dissipated through fluid shear and associated flow losses, or,

$$\frac{g\rho H}{g_c} + P_1 = \Delta P_f + 2\left(\frac{\rho\bar{u}^2}{2g_c}\right) + X \tag{3}$$

X denotes a probable loss due to particle slippage at tube walls when the fluid is a non-Newtonian suspension. This wall effect is thought to be small for concentrated, well dispersed, non-Newtonian fluids (*4, 7*). Vand (*14*) has investigated wall effects from a particle standpoint for suspensions of small glass spheres. Based on Vand's work an estimate of wall effects for our sample suspensions indicates a negligible factor with respect to the range of our experimental parameters; the slippage loss is neglected for this study. Fluid velocity in the reservoir is quite small compared with the velocity of the fluid in the capillary; consequently, Equation 3 above illustrates the means by which ΔP_f is obtained experimentally,

$$\Delta P_f = P_1 + \frac{g\rho H}{g_c} - \left(\frac{\rho\bar{u}^2}{g_c}\right) \tag{4}$$

P_1 and H are measured directly; $\bar{u}$ is calculated from volumetric flow data; and ρ is obtained through calculation (volume weighted densities or hydrostatic weighing).

The $(\rho\bar{u}^2/2g_c)$ losses as described above pertain strictly to Newtonian fluid flow. The velocity profile for dilatant flow rarely approximates a paraboloid. McMillen (*6*) has studied non-Newtonian flow entrance and kinetic energy losses in some detail for a Bingham plastic gel. These losses were six times greater than those of a corresponding Newtonian flow model. It was suggested that the relative increase in losses for non-Newtonian fluids was due to particle alignment at the tube entrance. There was little data available for confirmation of this theory. Bogue (*1*) has analyzed entrance losses for fluids of the power law type. Effective pressure losses varied only slightly from Newtonian fluid values if the flow behavior index did not differ greatly from unity. This was indeed the case for our range of experiments. For this study of dilatant suspensions conventional Newtonian flow losses were assumed where they were significant.

Capillaries of copper and a high nickel alloy were used with lengths varying from 13 to 16 inches. Sizing the capillaries was accomplished by measuring the volume of water necessary to fill them. Average diameters obtained in this manner differed from manufacturer's specifications by approximately 2%. The experimentally determined values, 0.0664, 0.0630, and 0.0511 inch, were used in subsequent calculations.

For the water runs there was little shear rate range available before the onset of turbulence, since the instrument was designed for high consistency suspensions. However, successful runs were made with water obeying the usual linear relation

$$\left(-\frac{du}{dr}\right)_w = \frac{\tau_w}{\mu} \tag{5}$$

The slope of the shear rate–shear stress curve is the viscosity of water. The experimentally determined viscosity differed from the accepted value by 0.8%. When calibrating with glycerine a larger range of flow rates was possible before the onset of turbulence because of its greater consistency, facilitating accurate viscosity measurements. The calibration runs established confidence in the reliability of the fluid shear data provided by the rheometer.

FLOW PROPERTIES OF SOME DILATANT MATERIALS.

The Metzner and Reed Model. Equations for describing fluid shear properties were employed in calibration computations. The general mathematical formulation of these equations is chiefly the work of Rabinowitsch (*11*) and Mooney (*9*). But, Metzner and Reed (*8*) have rearranged the equations, which basically relate rate of shear of a fluid to shear stress independent of fluid properties in such a manner that all non-Newtonian classifications of flow are treated in a perfectly rigorous fashion provided the mode of flow is laminar. The mathematical development is clearly revealed in references (*8*) and (*13*).

The analysis establishes a regrouping of the equations of Rabinowitsch and Mooney for wall shear rate to give,

$$\left(-\frac{du}{dr}\right)_w = \frac{3n'+1}{4n'} \cdot \frac{8\bar{u}}{D} \tag{6}$$

and for wall shear stress,

$$\tau_w = \frac{D\Delta P_f}{4L} = k'\left(\frac{8\bar{u}}{D}\right)^{n'} \tag{7}$$

If $\log (D\Delta P_f/4L)$ is plotted *vs.* $\log (8\bar{u}/D)$ the slope of this curve for any prescribed wall shear stress, τ_w, is given by n'. Using the corresponding $8\bar{u}/D$ values, where $8\bar{u}/D$

is the bulk shear rate, a characteristic flow curve, τ_w *vs.* $(du/dr)_w$, can be constructed with the aid of Equation 6 which will serve to identify dilatant fluid properties. Extrapolation of the logarithmic plot back to $8\ \bar{u}/D$ equal unity establishes the value of k'. As pointed out in the development of these equations by Metzner and Reed, no generality has been lost up to this point, and the equations rigorously apply to laminar flow of non-Newtonian and Newtonian fluids alike.

Therefore the parameters n' and k' are prime rheological constants necessary for characterization of flow. The "flow-behavior index" is represented by n' and its magnitude determines the degree of dilatancy. The "fluid consistency index," denoted by k', is proportional to the viscous resistance of the fluid sample. In most cases n' is constant over shear rate ranges of general interest; note that from Equation 7 at least two flow rates are necessary to calculate n' and k', and hence to establish dilatancy.

As pointed out by Metzner and Reed, if the flow-behavior index, n', is unity, then k' becomes μ and substituting Equation 6 into Equation 7:

$$\tau_w = \mu \left(- \frac{du}{dr} \right)_w \tag{8}$$

which is Newton's law for viscuous or "Newtonian" flow. If $n' > 1$ the flow is termed dilatant and if $n' < 1$ the flow is pseudoplastic.

The indexes n' and k' are known to change with variations of temperature and solids concentration (*7*). The flow behavior index, n', is slowly varying with temperature and will not change appreciably for small variations providing there is no reaction or mutual solubility between liquid and solid phases. The consistency index, k', will on the other hand vary about as rapidly as would the viscosity of a Newtonian liquid phase. The change in k' with temperature is an order of magnitude greater than changes in n'. For dilatant fluids n' is expected to increase with increases in solid concentration—i.e., increased dilatancy is expected until the material becomes too rigid to measure. The iron oxide data contradicts this statement. The constant, k', will again vary more rapidly than n' as the suspension is thinned down or thickened.

Experimental Results. The literature (*3*) has indicated ranges of volume per cent solids for particular materials within which dilatant flow may be expected to persist. Sample suspensions, prepared for the rheometer, are described below along with the test results. The pigments used in these experiments were finely divided powders of standard chemical reagent grade.

STARCH IN ETHYLENE GLYCOL. Several batches of starch and glycol were mixed. The ρ-glycol was given by the manufacturer; ρ-starch was found through volume-weight experiments to be within 2% of the theoretical value. Trial samples were too dense to use in the rheometer since under the slightest shear they would dry to a solid mass. Using the respective densities of starch and glycol, 1.511 grams/ml. and 1.114 grams/ml., a 35.0 vol. % starch suspension was formed. This was thought to be on the lower limit of dilatancy. The proper quantity of starch was weighed on an analytical balance for a given volume of glycol. The starch was stirred slowly into the glycol to avoid lumping. Another starch and glycol suspension was formed at 40.0 vol. % solids in a similar manner. Starch and glycol suspenions are fairly stable and settling was negligible for about one-half hour. Runs through the rheometer takes less than one hour ordinarily, so settling was only a minor uncertainty. Particle growth due to adsorption of liquid vehicle was small for these systems (*3*), so aging was not a serious factor. The age of both of the above mentioned starch suspensions was 1.5 hours.

Before placing the samples in the instrument, specific gravity measurements were performed. This was accomplished through hydrostatic weighing. Densities obtained in this manner differed from volume-weighted density calculations by less than 1%, and indication of good particle dispersion.

The starch samples were tested in the rheometer, and k' and n' were found by using Equation 7 for a given set of capillary dimensions and for a certain flow rate and pressurization. The parameter, n', is the slope of the respective curves in Figure 2. These indexes were used to calculate wall shear rate for each wall shear stress value. Equation 6 indicates this calculation.

The 35.0 vol. % solids sample data was limited but slight dilatancy is indicated as the curve bends toward the stress axis. Greater dilatancy is apparent for the 40.0 vol. % sample as was expected. Figure 3 depicts the results for these samples. The scatter of the 40.0 vol. % solids data is due to the volume-catch procedure that was initially employed. The weight-catch procedure was later found to yield data with better resolution. Table I presents data as compiled for plotting shear characteristics. Fischer (*3*) finds dilatancy in starch systems in the concentration range 42.4–50.8 vol. % solids, using a rotational viscometer, while in this study 35.0 vol. % solids is indicated as a lower limit for dilatancy.

RED IRON OXIDE IN AQUEOUS, SULFONATED LIGNIN SOLUTIONS. Iron oxide suspensions are not consistent with the dilatant theory of Reynolds (*12*) in that dilatancy is observed at relatively low solid volume percentages because of the asymetric shape of the particles. A 12.0 vol. % suspension was prepared, since dilatancy was expected at that concentration. To contrast this and in an effort to form a high consistency suspension another sample was mixed to give 26.2 vol. % solids. The iron oxide particles

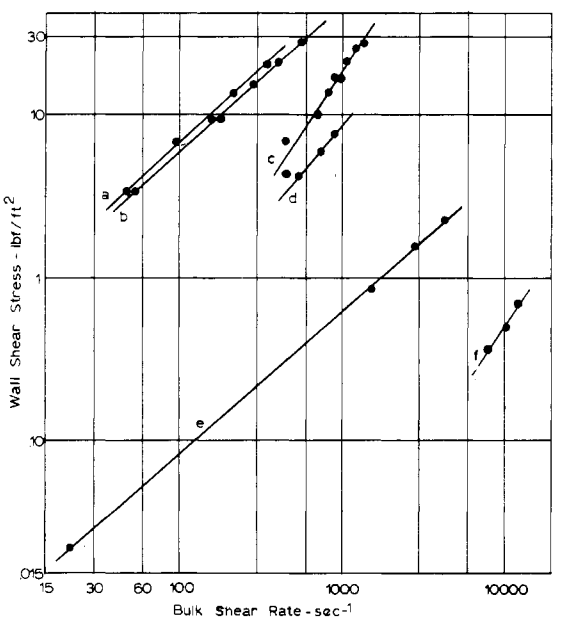

Figure 2. Bulk shear rate characteristics for all suspensions

a. Zinc oxide, 29.7 vol. % solid, $n' = 0.895$
b. Zinc oxide, 31.0 vol. % solid, $n' = 0.900$
c. Starch, 40.0 vol. %, $n' = 1.49$
d. Starch, 35.0 vol. %, $n' = 1.16$
e. Iron oxide, 26.2 vol. %, $n' = 0.875$
f. Iron oxide, 12.0 vol. %, $n' = 1.30$

Table I. Data for Plotting Shear Characteristics

Material	Concentration, % Vol.	Concentration, % Wt.	Age Hr.	Density ρ Lb. Mass/Ft.^{3}	Temperature °F.	n'	k' Lb. Force. Sec.$^{n'}$/Ft.^{2}	$(D\Delta P_f/4L)$ Lb. Force/Ft.^{2}	$(8\bar{u}/D)$ Sec.$^{-1}$	$(-du/dr)_w$ Sec.$^{-1}$
Starch in Glycol	40.0	47.4	1-½	78.7	78.0	1.488	6.44×10^{-4}	4.29	447	411
								6.85	445	408
								10.2	692	636
								13.6	810	744
								17.0	973	894
								21.3	1,054	969
								25.4	1,174	1,078
								27.7	1,339	1,230
								17.0	884	812
Starch in Glycol	35.0	42.5	1-½	78.3	76.0	1.156	0.00296	4.20	534	515
								5.97	736	711
								7.58	890	859
FeO in Lig. Soln.	26.2	63.4	½	131.7	77.5	0.875	0.00146	2.30	4,315	4,470
								0.0212	21.3	22.1
								0.858	1,529	1,585
								1.58	2,867	2,970
FeO in Lig. Soln.	12.0	40.2	⅓	95.5	80.5	1.304	2.98×10^{-6}	0.362	7,900	7,440
								0.702	13,050	12,280
								0.504	10,250	9,650
ZnO in Lig. Soln.	31.0	71.0	½	154.3	77.4	0.900	0.0942	3.43	53.9	55.4
								9.38	177	182
								15.34	278	286
								21.1	404	415
								27.9	558	574
								9.38	155	159
ZnO in Lig. Soln.	29.7	69.7	79-⅔	150.5	77.1	0.895	0.1118	3.41	47.0	48.4
								6.81	95.4	98.2
								13.6	212	218
								20.3	343	353

were apparently quite small and free of flocculation since even the 26.2 vol. % sample remained relatively fluid upon visual inspection. Iron oxide was dispersed in a 10 wt. % solution of sodium lignin sulfonate, a commercial surface active agent, "Marasperse N," supplied by The Marathon Corp., Menasha, Wis., where the lignin compound served as a dispersing agent. Settling was not a problem if the samples were tested as they were prepared. Specific gravity determinations were made as indicated above.

In determining the n' and k' values for the 12.0 and 26.2 vol. % iron oxide samples difficulty was encountered because of the highly fluid condition of the suspensions, i.e., the shear stress range was limited due to turbulence in the finest diameter capillary. However, n' and k' were found from the usual logarithmic plots when reliable data were obtained at both concentrations. These plots are shown in Figure 2. The wall shear rates were calculated from Equation 6 and these results appear in Figure 4. The data are tabulated in Table I.

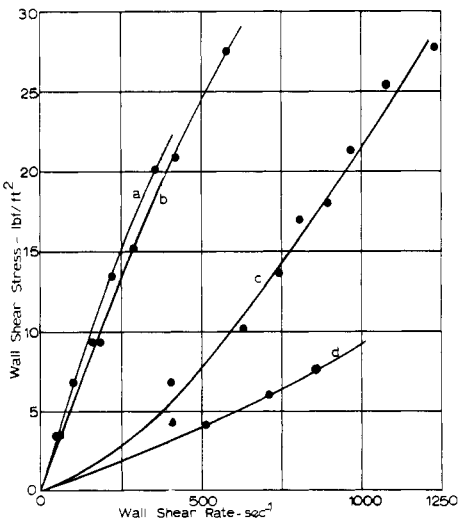

Figure 3. Wall shear rate characteristics for starch and zinc oxide suspensions

a. Zinc oxide, 29.7 vol. %, 77.1° F., age 79⅔ hrs.
b. Zinc oxide, 31.0 vol. %, 77.4° F., age ½ hr.
c. Starch, 40.0 vol. %, 78.0° F., age 1½ hrs.
d. Starch, 35.0 vol. %, 76.0° F., age 1½ hrs.

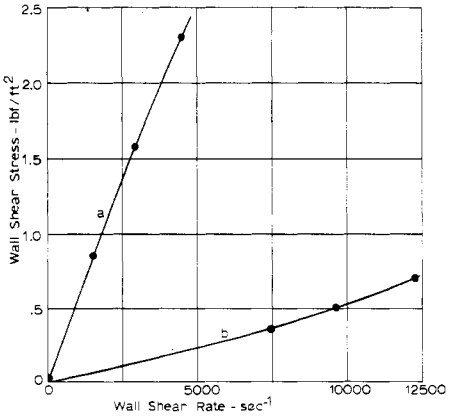

Figure 4. Wall shear rate characteristics for iron oxide suspensions

a. 26.2 vol. %, 77.5° F., age ½ hr.
b. 12.0 vol. %, 80.5° F., age ⅓ hr.

The literature quotes a narrow dilatancy range for iron oxide suspensions, 1 or 2% around 12.0 vol. %, and as expected the 12.0 vol. % solids sample indicated strong dilatancy. Upon doubling this concentration the iron oxide suspension exhibited slight pseudoplasticity as evidenced by n' being less than unity. This is curious since increasing solid concentration would usually enhance dilatant characteristics, but this anomalous quality of iron oxide suspensions was mentioned above.

ZINC OXIDE SUSPENDED IN LIGNIN SOLUTION. Zinc oxide suspensions are thought to flow as dilatants for solid volume concentrations of greater than 30%. This material will also show a time dependency with continued shearing of a sample; owing to a structural rearrangement, thixotropy is sometimes noticed. However, in the capillary rheometer, new material is constantly being sheared, hence the dilatancy of a concentrated suspension should be manifest despite thixotropy.

Settling presented no appreciable problem in the zinc oxide suspensions when the dispersing agent was employed. Daniel (2) presents a comprehensive discussion of zinc oxide suspensions, where dilatancy was used as a measure of particle dispersion.

Final zinc oxide samples were prepared having 29.7 and 31.0 vol. % solids. The effect of aging on the 29.7% sample was noted semiquantitatively. The rheological constants were measured after 19 hours and 79 hours; n' values were essentially the same, but k' increased 15% over the 60-hour aging period. Both zinc oxide samples were tested at essentially the same temperature, ambient. The volume-weighted density values were used for both concentrations (Table I).

The slope of the curves on the logarithmic plot in Figure 2 are the respective n' values. The constant, k', is calculated, where extrapolation is impractical, by selecting some arbitrary point on the log τ_w *vs.* log 8 $\bar{u}/D$ curves. Equation 6 defines the wall shear rate, $(-du/dr)_w$; and, results for each of the zinc oxide suspensions are shown in Figure 3. In obtaining this zinc oxide data, there was an effort to show a change in flow property, perhaps from pseudoplasticity to dilatancy as the assumed lower limit for dilatancy (about 30 vol. % solids) was crossed. A 32.9 vol. % solids suspension was prepared, but unfortunately this sample was too dry and immobile to flow through the rheometer.

Consistent with the definitions of pseudoplasticity and dilatancy, Figure 3 shows that the zinc oxide sample with greater solid volume displays a lower shear stress for a given wall shear rate while the opposite effect is noted for the dilatant starch suspensions in Figure 3.

CONCLUSIONS

This study has provided data which give some insight into flow behavior of dilatant suspensions; also indicated were various pitfalls encountered when an effort was made to establish reproducible flow conditions. The intent has been to provide additional data for the limited compilation of flow properties of non-Newtonian fluids and in particular dilatant suspensions, having in mind the needs of the hydraulic engineer.

ACKNOWLEDGMENT

This study was made possible through a fellowship awarded the author by the Westinghouse Electric Corp. and the United States Atomic Energy Commission in conjunction with the University of Pittsburgh. The author greatly appreciates the initial suggestions of George Sonneman of the University and the use of laboratory facilities in the Mechanical Engineering Department. Invaluable suggestions regarding the preparation of the manuscript were given by Frances M. Richardson of North Carolina State College.

NOMENCLATURE

- du/dr = velocity gradient or shear rate; referred to tube wall with subscript w, sec.$^{-1}$
- D = capillary diameter, ft.
- g = gravitational constant, 32.2 ft./sec.^{2}
- g_c = conversion factor, 32.2 lb. mass ft./lb. force sec.^{2}
- H = elevation head of fluid in rheometer, ft.
- k' = fluid consistency index (lb. force) (sec.$^{n'}$)/ft.^{2}
- L = capillary length, ft.
- n' = flow behavior index, dimensionless
- P_1 = pressure applied to induce flow, lb. force/ft.^{2}
- ΔP_T = pressure loss in laminar flow, lb. force/ft.^{2}
- ΔP_f = calculated friction pressure drop, lb. force/ft.^{2}
- r = distance along tube radius, ft.
- $\underline{u}$ = local velocity, ft./sec.
- $\bar{u}$ = bulk fluid velocity, ft./sec.
- X = pressure loss due to slippage at tube walls, lb. force/ft.^{2}
- μ = Newtonian viscosity lb. force sec./ft.^{2}
- ρ = density, lb. mass/ft.^{3}
- τ = shear stress, referred to the tube wall with subscript w, lb. force/ft.^{2}

LITERATURE CITED

(1) Bogue, D.C., *Ind. Eng. Chem.* **51**, 874–8 (1959).
(2) Daniel, F.K., *India Rubb. World* **101**, No. 4, 33 (1940).
(3) Fischer, E.K., "Colloidal Dispersions," Wiley, New York, 1950.
(4) Green, H., "Industrial Rheology and Rheological Structure," Wiley, New York, 1949.
(5) Handbook of Chemistry and Physics, Hodgman, C.P., ed., Chemical Rubber Publishing Co., Cleveland, 1953.
(6) McMillen, E.L., *Chem. Eng. Progr.* **44**, 537 (1948).
(7) Metzner, A.B., in "Advances in Chemical Engineering," T.B. Drew and J.W. Hooper, Jr., ed., Academic Press, New York, 1956.
(8) Metzner, A.B., Reed, J.C., *A.I.Ch.E. Journal* **1**, No. 4, 434–40 (1955).
(9) Mooney, M., *J. Rheology* **2**, No. 2, 210–22, (1931).
(10) Prandtl, L., Tietjens, O.G., "Applied Hydro- and Aero-Mechanics," McGraw-Hill, New York, 1934.
(11) Rabinowitsch, B., *Z. Physik. Chem.* **145A**, No. 1, (1929).
(12) Reynolds, O., *Phil. Mag.* **20**, 469 (1885).
(13) Roberts, A.S., Jr., M.S. thesis, University of Pittsburgh, Pittsburgh, Pa., June 1959.
(14) Vand, V., *J. Phys. Colloid Chem.* **52**, 300–14 (1948).

RECEIVED for review August 27, 1962. Accepted April 11, 1963.

CORRECTION:

In the article "Low Temperature Heat Capacity and Entropy of Basic Potassium Aluminum Phosphate" by Edward P. Egan, Jr., Zachary T. Wakefield, and Basil B. Luff [J. CHEM. ENG. DATA 8, No. 2, 184–5 (1963)] there is an error in Table II. The line of entries for 290° K. should be replaced by the two lines of entries.

290	74.99	68.32	11,180
300	76.87	70.90	11,940